

Chapter 2

Basic Color Theory

In this chapter I will give an introduction to two classical theories of color vision. Probably the most influential theory is the theory of trichromatic color vision which will be discussed first. In the second part I will examine characteristics of a subpopulation of observers called *dichromats*. The existence and the characteristics of these color deficient observers are well explained within the framework of trichromatic theory. The chapter will be concluded with an introduction to the second classical theory of color vision, the theory of opponent colors. This theory had been standing in opposition to trichromatic theory for many years. Now it is commonly accepted that the two theories refer to different stages of color processing in the visual system.

2.1 Primary Color Coding

The theory of trichromatic color vision was mainly developed in the 19th century and is closely connected with the names of Thomas Young, Hermann von Helmholtz, James Clerk Maxwell and Hermann Grassmann. The enormous success of the theory results especially from the fact that the theory of trichromatic color vision provides an adequate description of processing of light at retinal level. Furthermore, conclusions derived from the theory play an important role in most applications that deal with color vision. In particular, quantitative aspects of the theory constitute the foundations of the field of *colorimetry* that these applications are based on.

The main goal of the theory of trichromatic color vision is to connect characteristics of the physical stimulus of light, that is electromagnetic radiation within the visible spectrum, with the matching behavior of observers which is determined by psychological variables. The physical stimulus—light—can be characterized by its spectral power distribution within the visible spectrum (Figure 2.1). In the following I will describe how the relation between the physical stimulus and the psychological percept is conceptualized and ‘measured’ within the framework

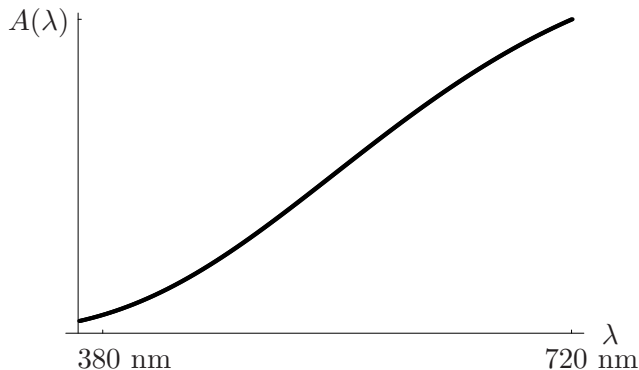


Figure 2.1: Spectral power distribution of a tungsten light source A .

of trichromatic theory. This relation can be understood as a mapping from the physical world to psychological sensations.

2.1.1 The Experimental Paradigm

In classical experiments of trichromatic theory subjects are presented with two lights a and b on the two halves of a bipartite disk (Figure 2.2a).¹ The task of the subject is to change light b in color appearance until it is perceptually indistinguishable to light a on the other half of the disk. This criterion of perceptual indistinguishability is called *metamerism* and is written $a \sim b$. Properties of the relation of metamerism are reflexivity, symmetry and transitivity. Therefore metamerism is an equivalence relation which is only defined by a psychological criterion. In other words, two lights that are metamers generally differ in their spectral power distributions. The classical color matching experiments are based on two *physical* operations, namely the additive mixture of lights (\oplus) and scalar multiplication ($*$). In practice additive mixture is realized as superposition of lights whereas scalar multiplication can be understood as change of the intensity of lights. These operations allow us to define linear combinations of lights m_1, m_2, m_3 with intensities t_1, t_2, t_3 :

$$t_1 * m_1 \oplus t_2 * m_2 \oplus t_3 * m_3. \quad (2.1)$$

In the experiment, the light b is replaced with such a linear combination of three lights on the right half of the disk (Figure 2.2b). The subject is asked to adjust the intensities t_1, t_2, t_3 of the three *independent* basis lights until the

¹Two restrictions on the experimental conditions are usually made. First, the stimulus is presented against a black background. Second, the size of the disk is limited to two degrees of visual angle to yield only foveal stimulation.

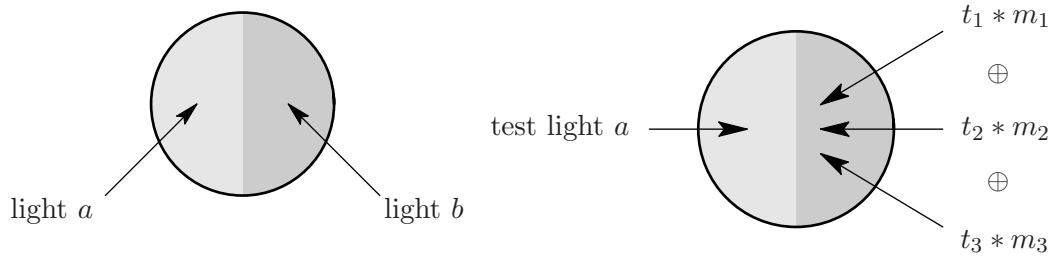


Figure 2.2: (a) Presentation of two lights a and b on the two halves of a bipartite disk (left). (b) Configuration in the classical color matching experiment. Light a is matched with a mixture of lights m_1, m_2, m_3 (right).

mixture is metamer to a given test light a on the left half of the disk.² This procedure is called *color matching*. In general, subjects need just three basis lights to find a color match for any given test light a . Each test light can be characterized by the three numbers t_1, t_2, t_3 , which we will later refer to as *color codes*.³ This fundamental characteristic of human color vision is called *trichromacy*. In contrast, some observers need only two basis lights to find a color match for any given test light. These observers are called *dichromats*. We will come back to this point later in this chapter.

2.1.2 The Grassmann Laws

Grassmann (1853) put results from color matching experiments in a formal theoretical framework. He expressed three characteristics of metamerism that define the space of lights as an infinite vector space. These fundamental conclusions are known as *Grassmann laws*. Given three lights a, b, c and scalars $t \geq 0$, the following equations hold for the metamerism relation:

$$a \sim b \Leftrightarrow a \oplus c \sim b \oplus c, \quad (2.2)$$

$$a \sim b \Leftrightarrow t * a \sim t * b. \quad (2.3)$$

The third of Grassmann's laws is the already mentioned trichromacy of normal human observers. Empirical work has shown that the Grassmann laws generally hold. An axiomatic formulation of the Grassmann theory is given in Krantz (1975).

²The term *independent basis lights* refers to the claim that each of the basis lights can not be represented as a mixture of the two other basis lights.

³For some test lights it is impossible to find a satisfying match using the method just described. In this case one of the three basis light is presented on the half of the test light. Using this indirect color matching procedure the subject is asked to adjust the three intensities t_1, t_2, t_3 until both halves are indistinguishable in color appearance.

2.1.3 Primary Color Codes

If we choose a fixed set of three basis lights, we can define each test light a by the three numbers t_1, t_2, t_3 that are needed to match a with the mixture of the three basis lights m_1, m_2, m_3 . This triple of numbers is called *primary color code* or *tristimulus values* and we will denote it with the vector $\mathbf{t} := (t_1, t_2, t_3)'$. Lights that are metamers have identical primary color codes and lights with identical color codes are perceptually indistinguishable:

$$a \sim b \Leftrightarrow \mathbf{t}^a = \mathbf{t}^b. \quad (2.4)$$

The primary color code t_1^a, t_2^a, t_3^a of a given light a is a linear function of the spectral power distribution of that light. Together with (2.2) and (2.3) the space of color codes is therefore defined as a three dimensional vector space. This means that

$$\mathbf{t}^{a \oplus b} = \mathbf{t}^a + \mathbf{t}^b \quad (2.5)$$

and

$$\mathbf{t}^{s \cdot a} = s \cdot \mathbf{t}^a \quad (2.6)$$

hold for all lights a, b and scalars $s \geq 0$. Imagine we were able to carry out the color matching experiment with a fixed set of basis lights and determine primary color codes for all possible lights as test lights. If we represent all obtained color codes in three dimensional vector space the result would be a geometric structure that is called *color cone* (Figure 2.3). The color cone can also be interpreted as the mapping of all realizable lights (which are a subset of infinite vector space) onto a three dimensional vector space which we will refer to as *color space*.⁴

Usually the basis lights that are used in the color matching experiment are narrow band lights with a bandwidth of only one nanometer. These lights are called *spectral lights* and they are characterized by the respective wavelength number. The set of spectral lights with unit radiant power $\{e_{300}, \dots, e_{700}\}$ is called *equal energy spectrum*. For each of these spectral lights e_λ the spectral power distribution $e_\lambda(x)$ is 1 if $x \in [\lambda - \frac{1}{2}; \lambda + \frac{1}{2}]$ and else 0. Later the spectral power distribution of a given light will be approximated using the equal energy spectrum.

A common set of basis lights is the *RGB-system*. The three basis lights of this system appear reddish ('R', 700 nm), greenish ('G', 546 nm) and bluish ('B', 436 nm) to the normal observer.⁵ If we want to determine the primary color code of a given light a regarding to the three basis vectors R, G, B we could carry out the color matching experiment. Now a more convenient method to obtain the intensities t_1^a, t_2^a, t_3^a for a given light a without conducting the color matching experiment will be described. First, we determine experimentally the

⁴Note that the color cone is a subspace of color space which contains tristimulus values of all physically realizable lights.

⁵Note that the color codes of the three basis lights must lie within the color cone

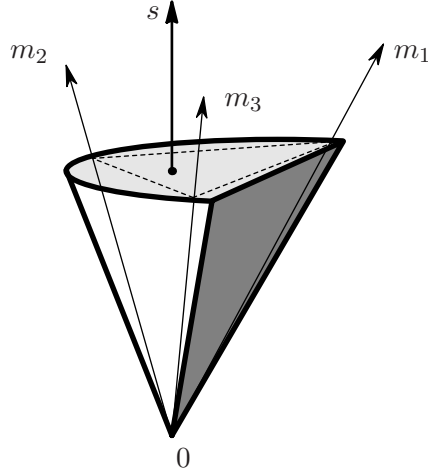


Figure 2.3: The color cone and the three basis lights m_1 , m_2 and m_3 .

tristimulus values of all spectral lights e_λ of the equal energy spectrum using e_{700} , e_{546} and e_{436} as basis lights. As a result we get mean tristimulus values \bar{t}_1^λ , \bar{t}_2^λ , \bar{t}_3^λ for each spectral light λ across several observers. These mean intensities can be denoted as three functions $\bar{r}(\lambda)$, $\bar{g}(\lambda)$, $\bar{b}(\lambda)$ of the wavelength λ and are called *color matching functions* (Figure 2.4). In the next step we can approximate the spectral power distribution of a given light a as linear combination of the equal energy spectrum with $a(\lambda)$ as coefficients:

$$a \sim \sum_{\lambda=300}^{700} a(\lambda) * e_\lambda. \quad (2.7)$$

Given this approximation and the relations (2.5) and (2.6) we get the tristimulus values of the light a with

$$\mathbf{t}(a) = \sum_{\lambda=300}^{700} a(\lambda) \cdot \mathbf{t}^{e_\lambda}. \quad (2.8)$$

As we used the color matching functions $\bar{r}(\lambda)$, $\bar{g}(\lambda)$, $\bar{b}(\lambda)$ to denote the tristimulus values of all spectral lights e_λ we can also write

$$\begin{aligned} t_1^a &= \sum_{\lambda=300}^{700} a(\lambda) \cdot \bar{r}(\lambda), \\ t_2^a &= \sum_{\lambda=300}^{700} a(\lambda) \cdot \bar{g}(\lambda), \\ t_3^a &= \sum_{\lambda=300}^{700} a(\lambda) \cdot \bar{b}(\lambda). \end{aligned} \quad (2.9)$$

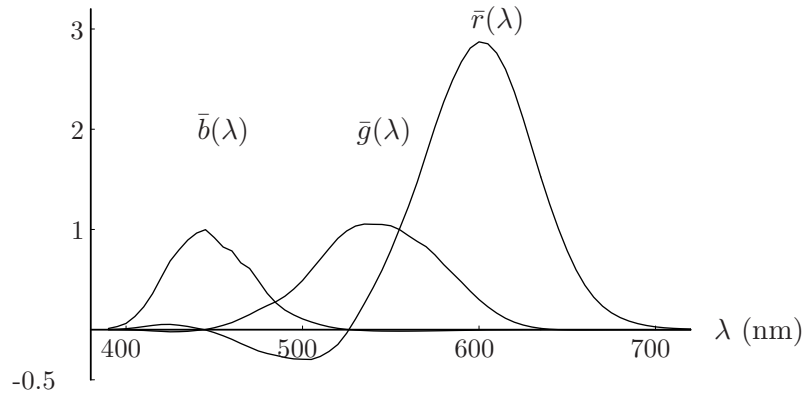


Figure 2.4: Color matching functions $\bar{r}(\lambda)$, $\bar{g}(\lambda)$ and $\bar{b}(\lambda)$ of the CIE-1931 standard observer.

If the color matching functions for a given set of basis lights are known, the color codes of any light a can be computed easily.

One disadvantage of the *RGB*-System is that—since the color codes of the basis lights are part of the color cone—for some lights, negative coefficients result. If we prefer a set of basis lights which provides only positive coefficients the color codes of these ‘basis lights’ must lie necessarily outside the color cone. It is evident that in this case the basis of such a system is constituted by not realizable ‘lights’.

An alternative system with this characteristic is the *CIE-XYZ-system* of the *Commission Internationale de l’Eclairage (CIE)*. In this coordinatization the basis vectors X , Y and Z are not part of the color cone and cannot be related with physical lights. As a consequence, for any given light only positive *XYZ*-tristimulus values result (Figure 2.5).

Another advantage of the *XYZ*-system is that the Y -coordinate is defined as the *luminance* of the light. Before we continue I will introduce the concept of luminance in brief. Roughly speaking, luminance corresponds to perceived brightness. The luminance $L(a)$ is defined as a linear function of the light a so that

$$L(a \oplus b) = L(a) + L(b) \quad (2.10)$$

and

$$L(s * a) = s \cdot L(a) \quad (2.11)$$

hold for all lights a , b and and scalars $s \geq 0$. As a consequence, all lights with identical luminance lie on a plane in color space. Analogous to the three color matching functions there is function of λ which is related to luminance. It is called the *luminous efficiency function* $V(\lambda)$ (Figure 2.6). The function $V(\lambda)$ can be also interpreted as a sensitivity function of human daylight vision. The luminance of a light is simply the integral of the product of $a(\lambda)$ and $V(\lambda)$ over

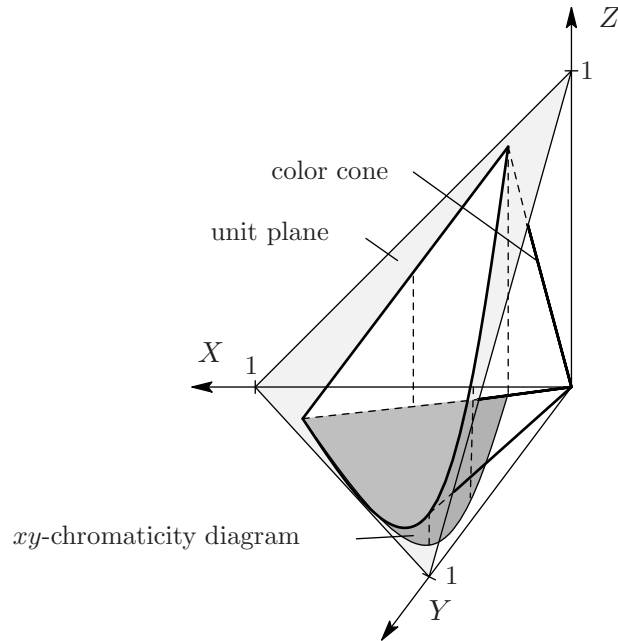


Figure 2.5: The *CIE-XYZ*-system and the color cone. The *xy*-chromaticity diagram can be interpreted as the projection of the unit plane onto the *XY*-plane.

the visible spectrum:

$$L(a) = \int_{\lambda} a(\lambda)V(\lambda) d\lambda. \quad (2.12)$$

Experimentally, $V(\lambda)$ is determined using a technique called *heterochromatic flicker photometry*.⁶ Two spectral lights are presented to the observer in rapid interchange at the same location. At a certain frequency of presentation differences in luminance of both stimuli are perceived as flicker whereas chromatic differences are not detectable for the visual system. This phenomenon has to do with the fact that the temporal resolution of the luminance path is finer than those of the chromatic paths. In the flicker experiment, one of the stimuli serves as a fixed standard which is usually the spectral light e_{555} . The task of the observer is to adjust the intensity of the other stimulus, the test light, until perceived flicker is canceled or minimized. If this procedure is done with all spectral lights as test lights, the resulting intensities m_{λ} can be expressed in relation to the intensity m_{555} of the standard. This yields to the luminous efficiency function $V(\lambda)$:

$$V(\lambda) = m_{555}/m_{\lambda}. \quad (2.13)$$

⁶As an alternative one might suggest to determine equally bright stimuli using equal brightness judgments. Unfortunately this method does not lead to a measure which is a linear function of the physical stimulus (Wyszecki & Stiles, 1982).

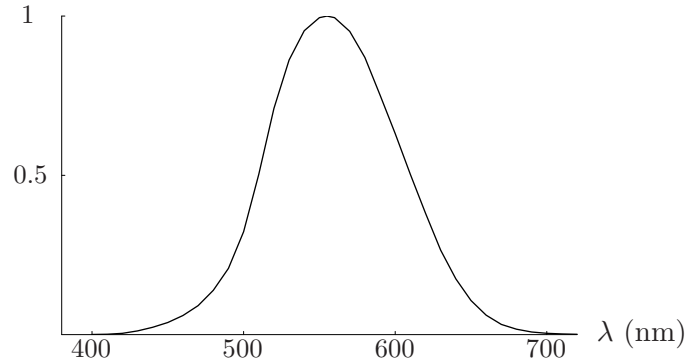


Figure 2.6: The luminous efficiency function $V(\lambda)$.

The *RGB*- and the *XYZ*-system can be both interpreted as coordinatizations of the three dimensional color space with different basis vectors. Therefore the transformation from one system to the other is simply given by multiplication with the respective 3×3 -transformation matrix. A two dimensional representation of chromaticities within the *CIE-XYZ-system* is the *xy-chromaticity diagram* (Figure 2.5 and Figure 2.7). The *xy*-chromaticity coordinates can be easily transformed from given *XYZ*-coordinates:

$$x = \frac{X}{X + Y + Z} \quad \text{and} \quad y = \frac{Y}{X + Y + Z} \quad . \quad (2.14)$$

Several efforts have been made to construct a transformation of color space which is based on perceptual distances. The *CIE* has suggested two systems that claim this purpose, the *CIE-Lab-system* and the *CIE-Luv-system*. Both coordinatizations are given by non-linear transformations of color space and depend on a reference light that refers to the adaptational state of the observer. However, none of the two systems provides an adequate representation of perceptual differences in terms of Euclidean distances. The chromaticities of the *CIE-Luv-system* are represented in the *u'v'*-diagram which is commonly used for data analysis and representation (Figure 2.7).⁷ An important feature of the *u'v'*-diagram is that straight lines in the *xy*-chromaticity diagram remain straight in the *u'v'*-diagram. The non-linear transformation from *xy*- to *u'v'*-coordinates is given by:

$$u' = \frac{4x}{-2x + 12y + 3} \quad \text{and} \quad v' = \frac{9y}{-2x + 12y + 3} \quad . \quad (2.15)$$

⁷The *u'v'*-diagram is often referred to as the *CIE 1976 UCS (uniform-chromaticity-scale)* diagram.

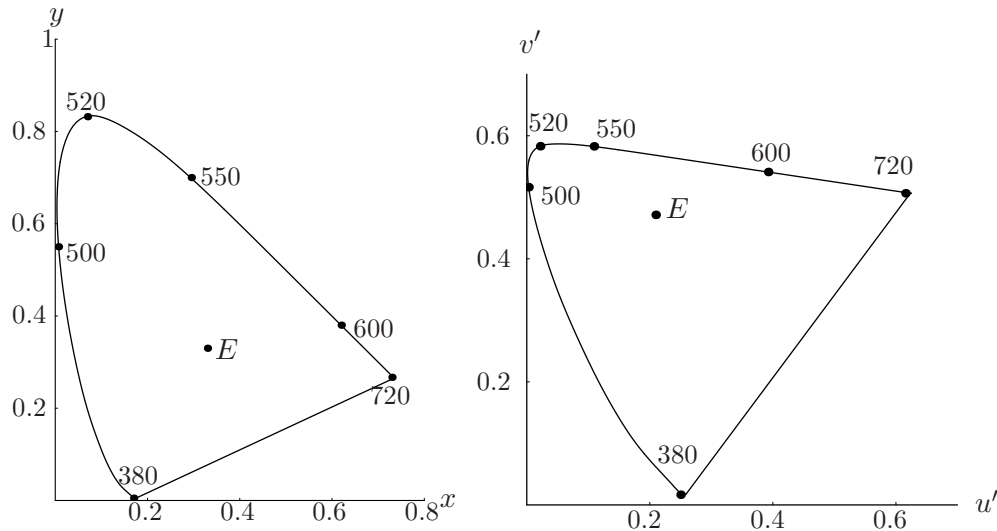


Figure 2.7: The xy -chromaticity diagram (left) and the $u'v'$ -chromaticity diagram (right) with the chromaticity of the equal energy spectrum (E) and selected spectral lights.

2.1.4 Receptor Codes

The finding from color matching experiments that most human observers need exactly three basis lights to find a color match to any given test light led to the conclusion that the matching behavior of observers is mediated by three different classes of photoreceptors that are often called *cone fundamentals*.⁸ These classes of photoreceptors differ in the spectral region of their maximal sensitivity. The first photoreceptor (L) has its maximal sensitivity in the longwavelength region of the spectrum, the second photoreceptor (M) is maximally sensitive in the middlewavelength region and the third photoreceptor (S) has its maximal sensitivity in the shortwavelength region of the spectrum.

At the time the theory of trichromacy was formulated first, the sensitivities of the photoreceptors were unknown. Therefore, one of the main challenges of trichromatic theory was to obtain functions that represent sensitivities of these assumed photoreceptors. The psychophysical determination of these sensitivity functions was first done by König and Dieterici (1893). Their work was based on two main assumptions. First, König and Dieterici assumed that a coordinatization of color space exists in which axes are represented by the three classes of photoreceptors. Second, they supposed that three classes of dichromats exist which differ in their matching behavior. Each of these classes of dichromats can

⁸The human retina contains a fourth class of photoreceptors that are called *rods*. The rods are extremely sensitive to light so that only one quantum of light is sufficient to excite a single rod (Hecht, Schlaer & Pirenne, 1942). Hence, rods mediate vision at very low light levels which is called *scotopic vision*. It is assumed that rods do not contribute to *photopic* daylight vision (Wyszecki & Stiles, 1982).

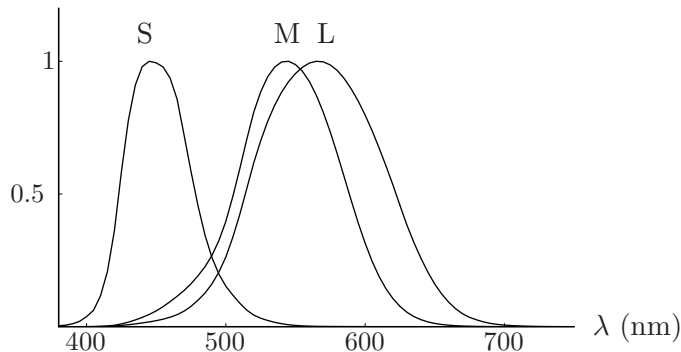


Figure 2.8: Sensitivity functions of the three photoreceptor classes L, M and S after Smith and Pokorny (1975). In this graph the functions are normalized to maximum value 1.

be characterized by the lack of one class of photoreceptors.

As a consequence of these assumptions, two lights that are perceptually indistinguishable for a given type of dichromat but in fact do not match for a normal trichromat can only differ in the excitation of the missing fundamental. If we present a given dichromat with a fixed test light in the color matching experiment, the color codes of the lights which are indistinguishable from the test light for that dichromat lie on a line in color space. Such a line is called *confusion line* of the respective dichromat. The lights whose color codes are aligned on a confusion line of a given dichromat differ only in the excitation of the missing photoreceptor of that dichromat. Hence confusion lines of a dichromat are parallel to the axis of the missing fundamental. König and Dieterici determined several confusion lines for each of the three classes of dichromats and shifted these lines to the origin of color space. The three resulting axes can be interpreted as a basis of color space which is related to cone excitations. The sensitivity functions of the three classes of photoreceptors can be obtained as a linear transformation of the color matching functions. It is worth noting that König and Dieterici's estimates of the sensitivity functions based on psychophysical experiments are in good agreement with physiological measurements that were done in the second half of the 20th century (e.g. Schnapf, Kraft & Baylor, 1987). Figure 2.8 shows sensitivity functions that were determined by Smith and Pokorny (1975). These estimates of the cone fundamentals will be used throughout this work.

Now we can characterize each light a by a triplet of numbers $\phi(a) = (\phi_1(a), \phi_2(a), \phi_3(a))$ that gives the photoreceptor excitations for this light. We will refer to this triplet of cone excitations as *LMS-* or *receptor codes*. If we denote the three sensitivity functions with $R_1(\lambda)$, $R_2(\lambda)$, $R_3(\lambda)$, the receptor codes of any given light a can be simply determined by

$$\phi_i(a) = \int_{\lambda} a(\lambda) \cdot R_i(\lambda) d\lambda, \quad i = 1, 2, 3. \quad (2.16)$$

The function ϕ can be interpreted as a linear mapping from the infinite space

of lights onto the three dimensional vector space which basis is given by the sensitivities of the three classes of photoreceptors⁹. This space is called *LMS- or photoreceptor excitation space*. Transformations to and from other coordinatizations of color space (*RGB, XYZ*) are simply given by respective 3×3 transformation matrices. In Equation (2.4) we already noted that two metameric lights a and b will be mapped to identical tristimulus values and vice versa. The same is true for receptor codes:

$$a \sim b \Leftrightarrow \phi(a) = \phi(b). \quad (2.17)$$

Here the psychophysical relation of metamerism is linked with the neurophysiological structure of cone photoreceptors. Therefore will refer to Equation 2.17 as *linking proposition*.

2.2 Dichromacy

In the following section we will focus on certain characteristics of dichromats. This subpopulation of color deficient observers differs in several respects from normal observers.

2.2.1 Dichromatic Color Spaces

We already defined dichromats as observers who need exactly two basis lights to find a color match for any given test light. As a consequence of this matching behavior, it was supposed that one class of photoreceptors is missing in dichromats. Given this assumption, three classes of dichromats can be distinguished: *protanopes*, which lack the *L*-cone, *deutanopes*, where the *M*-cone is missing and *tritanopes* which lack the *S*-cone. The three classes of dichromats differ in their adjustments in the color matching experiment. Therefore we will denote matches of each class by corresponding relations of metamerism \sim_P , \sim_D and \sim_T . Trichromatic matches are accepted by dichromats (König & Dieterici, 1893). As a consequence, the relation \sim is a subset of each and every dichromatic relation of metamerism:

$$\sim \subset (\sim_P \cap \sim_D \cap \sim_T). \quad (2.18)$$

In the last section I introduced a representation of color space that is given by photoreceptor excitations (ϕ_1, ϕ_2, ϕ_3) . As dichromats lack one type of cone photoreceptor, it is sufficient for them to characterize each light only by a pair of numbers which gives excitations of the two remaining cones. For example, in the protanope case we can denote this pair of numbers ϕ^P as

⁹The physically realizable lights constitute a *convex cone* within infinite vector space. Roughly speaking, a convex cone is a subset C of a vector space V where scalar multiplication is only allowed for positive scalars. The function ϕ can be understood as a linear mapping from this convex cone onto a convex cone in photoreceptor excitation space.

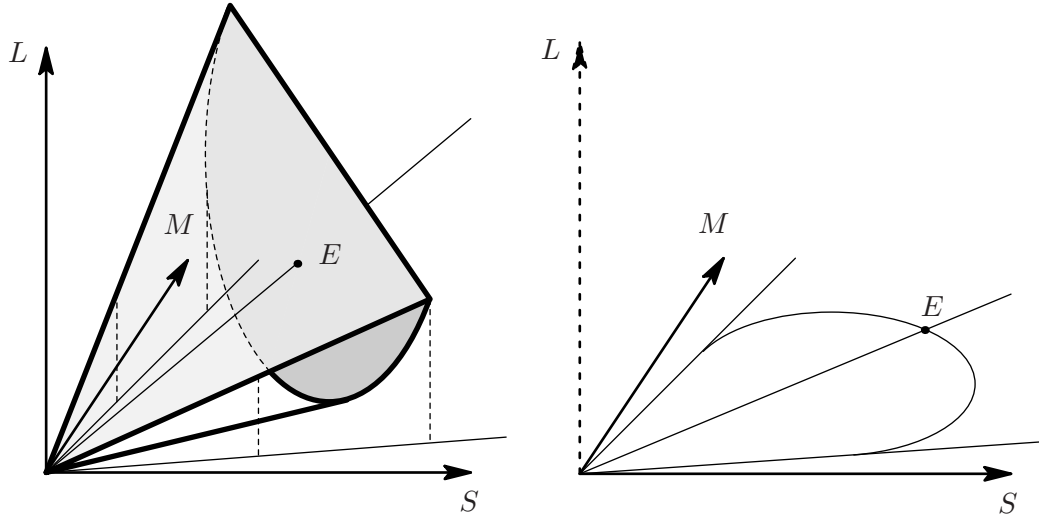


Figure 2.9: Cone excitation space of protanopes as a projection of the trichromatic color cone onto the MS -plane.

$$\phi^P(a) = (\phi_2(a), \phi_3(a)), \quad (2.19)$$

where $\phi_2(a)$ and $\phi_3(a)$ are receptor codes of the remaining cones. Hence dichromatic color spaces can be represented as two dimensional vector spaces.¹⁰ Analogous to the trichromatic case we can state a dichromatic linking proposition, which connects metamerism and receptor codes:

$$a \sim_P b \Leftrightarrow \phi^P(a) = \phi^P(b) \Leftrightarrow (\phi_2(a), \phi_3(a)) = (\phi_2(b), \phi_3(b)). \quad (2.20)$$

If in addition the lights a and b are distinguishable for normal trichromats so that $\phi_1(a) \neq \phi_1(b)$ the receptor codes of these two lights lie on a confusion line in trichromatic color space. This confusion line is parallel to the axis of the missing cone. I already mentioned that König and Dieterici (1893) used this fact when they estimated sensitivity functions of the three cone photoreceptors. If we visualize the two dimensional dichromatic cone excitation space, this space is defined as an orthogonal projection of trichromatic LMS -space. This projection is parallel to the missing receptor axis onto the plane which is spanned by the two remaining fundamentals (Figure 2.9). In this sense, the protanopic cone excitation space is given by the MS -plane, the deuteranopic space by the LS -plane and the tritanopic space by the LM -plane.

2.2.2 Classes of Dichromats

We already introduced the three different classes of dichromats protanopes, deuteranopes and tritanopes that are characterized by the absence of the L -, M - or

¹⁰The function ϕ^P can be interpreted as the linear mapping from the infinite space of lights to the two dimensional color space of protanopes.

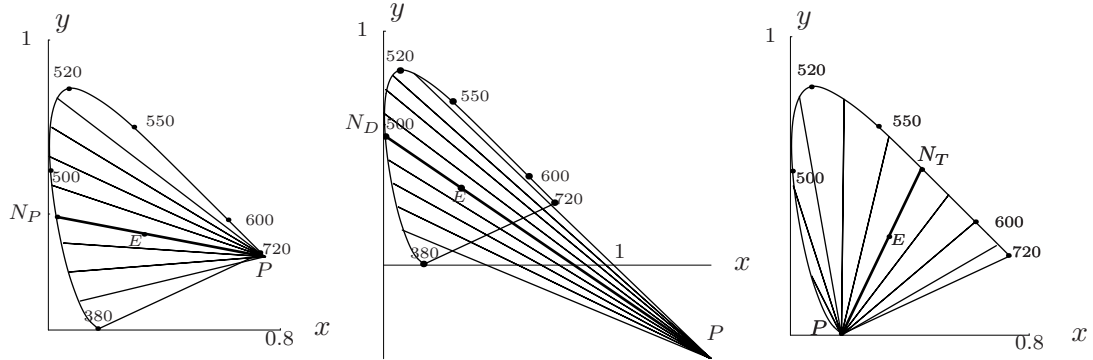


Figure 2.10: Pattern of confusion lines of protanopes (left), deuteranopes (center) and tritanopes (right) in xy -chromaticity diagram with confusion points (‘P’) and neutral points (‘N’). ‘E’ denotes the chromaticity of an equal energy spectrum.

S -photoreceptor respectively. Roughly speaking, protanopes and deuteranopes can be identified with red-green color blinds and tritanopes with blue-yellow color blinds. In the preceding section we discussed differences between types of dichromats that referred to confusion lines, relations of metamerism and color space. In this section I will introduce further distinctive characteristics of the three classes of dichromats.

We can define a plane in color space which contains tristimulus values of all lights b with:

$$a \sim_P t * b, \tag{2.21}$$

for scalars $t \geq 0$ and any fixed light a . These lights are metamers for protanopes except for intensity changes. Additionally, each of such planes contains all colors with receptor codes $t \cdot (\phi_1, 0, 0)'$. Hence, in the case of protanopes the intersection line of all these planes is the L -cone axis. If we picture these planes in xy -chromaticity diagram, each of the planes is represented by a confusion line. These patterns of confusion lines are distinctive for each class of dichromats. Figure 2.10 shows the patterns of confusion lines of the three types of dichromats in xy -chromaticity diagram. The confusion lines intersect at a specific point, the *confusion point*. This point has a clear geometrical interpretation. It is the point where the missing fundamental crosses the XYZ -unit plane. Protanopes, deuteranopes and tritanopes differ in their specific confusion points which are given in Table 2.1. Another distinctive feature of different classes of dichromats are *neutral points*. If we present an isolated stimulus which corresponds with an equal energy spectrum (‘E’ in Figure 2.10) to normal observers it will appear achromatic to them. For a given dichromat all stimuli that are metamer to this stimulus lie on a confusion line that crosses ‘E’. Consequently, there is also a spectral light that can be matched with white light by this dichromat and hence appears achromatic to him. The wavelength of this spectral light is the neutral

Table 2.1: Wavelengths of neutral points and xy -coordinates of confusion points of protanopes, deuteranopes and tritanopes (after Wyszecki & Stiles, 1982).

| dichromat | confusion point | neutral point |
|-------------|--------------------------|---------------|
| protanope | $x = 0.747$ $y = 0.253$ | 490 - 495 nm |
| deuteranope | $x = 1.400$ $y = -0.400$ | 495 - 505 nm |
| tritanope | $x = 0.171$ $y = 0$ | 568 - 570 nm |

point of this dichromat. The three types of dichromats can be also characterized by their respective neutral points which are given in Table 2.1.

Protanopes, deuteranopes and tritanopes differ also in their respective luminance functions. As explained above, only the L - and the M -cones contribute to the luminance function $V(\lambda)$ of color normal observers. Hence the luminance function of tritanopes $V_T(\lambda)$ is identical to that of normal trichromats. For protanopes only the M -cones contribute to luminance. The protanopic luminous efficiency function $V_P(\lambda)$ coincides with the sensitivity function of the M -cone photopigment. In the same way the luminosity function of deuteranopes is identical with the sensitivity function of the L -photoreceptor (Figure 2.11).

2.2.3 Diagnostics of Color Vision Deficiencies

Several diagnostic methods have been developed to detect color vision deficiencies. The most common instrument are pseudoisochromatic plates such as the Ishihara plates (Ishihara, 1997). These plates consist of a pattern of colored dots. Subjects are asked to detect a target which differs in color appearance from the background. The targets are normally letters or numbers. While tests based on pseudoisochromatic plates claim to discriminate reliably between different kinds of color deficiencies, inaccuracies in construction and in printing make them a choice for a first screening only.

The *anomaloscope* is a device which is used to classify different types of another group of color deficient observers, *anomalous trichromats*. In color matching experiments, anomalous trichromats need three basis lights to find a match for any given test light a . Hence the retina of those observers contains three different types of cones but the sensitivity function of one type of photoreceptors is shifted along the visible spectrum. The main forms of anomalous trichromacy are *protanomaly*, where the L -cone is modified and *deuteranomaly* where the M -cone is different from normal. For both classes of observers the ability to discriminate between spectral lights in the middle and long wavelength region is limited. Using the anomaloscope, the observer is presented with a mixture of two spectral lights, namely e_{535} and e_{670} which appear green and red to normal observers re-

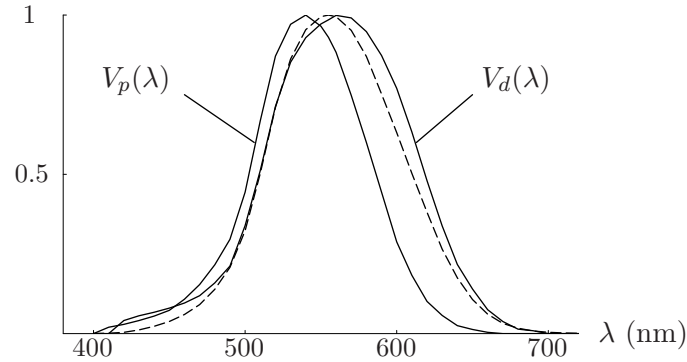


Figure 2.11: Luminosity functions of protanopes $V_p(\lambda)$ and deuteranopes $V_d(\lambda)$. The luminosity function of normal trichromats $V(\lambda)$ is shown in dashed line.

spectively. Then he is asked to match this mixture to a spectral light e_{589} that appears yellow to normal observers:¹¹

$$e_{589} \sim \alpha * e_{670} \oplus \beta * e_{535}. \quad (2.22)$$

The intensities α and β that provide a satisfying match constitute the *Rayleigh-ratio* R :

$$R = \frac{\alpha}{\beta}. \quad (2.23)$$

The test light e_{589} is chosen so that for normal observers $\alpha = \beta$ and hence $R = 1$ results. Protanomalous observers need a greater amount of the long wavelength light e_{589} for a satisfying match which means that for them $R > 1$. The Rayleigh ratio of deuteranomalous is smaller than one as they need a higher intensity β for their matches. The Rayleigh ratios of dichromats vary unsystematically over a wide range as they generally find a match when they are allowed to change only one of the two intensities.

A psychophysical approach to classify dichromatic observers is to obtain corresponding confusion lines. The most prominent example of this method is the pioneer work of König and Dieterici (1893) which was already reported in the previous section. In Chapter 4 I will describe a variation of this approach in detail that was used in the present study to classify dichromatic subjects.

2.2.4 Genetics of Color Vision Deficiencies

In former times it had already been noticed that color vision deficiencies are congenital and handed from one generation to the next. Now it is a well established fact that color vision defects have a molecular genetics basis (Nathans,

¹¹Note that the three spectral lights e_{535} , e_{670} and e_{589} are *not* independent mixture lights as it is generally claimed in color matching experiments. Their chromaticities lie on a line in xy -chromaticity diagram (see Figure 2.5) which indicates that all spectral lights on that line can be expressed as a mixture of only two of these spectral lights.

Table 2.2: Incident rates and genetics of color vision deficiencies (after Pokorny, Smith, Verriest & Pinckers, 1979; Wyszecki & Stiles, 1982).

| defect | incident rate (%) | | genetics |
|---------------|-------------------|-------|--------------------|
| | men | women | |
| protanopia | 1.0 | 0.02 | recessive X-linked |
| deutanopia | 1.1 | 0.01 | recessive X-linked |
| tritanopia | 0.002 | 0.001 | dominant autosomal |
| protanomaly | 1.0 | 0.02 | recessive X-linked |
| deuteranomaly | 4.9 | 0.38 | recessive X-linked |

Piantanida, Eddy, Shows & Hogness, 1986). More precisely, genetical analyses have shown that the *L*- and *M*-cone photopigments are encoded by genes that lie on the X-chromosome. As color vision deficiencies related to these cones are much more frequently observed in men than in women, it was supposed that protan and deutan defects are inherited as sex-linked recessive characteristics. In contrast, inherited tritan defects are rare and are not sex-linked. Table 2.2 gives an overview of the incident rates and genetics of the color vision deficiencies discussed here. Results from recent studies have shown that the patterns and variations of the underlying genetics are more complex than expected given only an examination of the phenotypes (Neitz, Neitz, He & Shevell, 1999; Neitz & Neitz, 2000).

2.2.5 Recent Results

Until this point we discussed dichromacy from the classical perspective which considers dichromatic vision as a reduced form of normal trichromatic vision. We will refer to this view as the *reduction hypothesis* of dichromatic color vision. According to this hypothesis, dichromatic color spaces are understood as two dimensional subspaces of the three dimensional trichromatic color space. However, several results from a number of recent studies are contradictory to the reduction hypothesis. A typical finding is that dichromats use the whole range of color terms when asked to describe their color percepts (Scheibner & Boynton, 1968; Montag, 1994; Paramei, Bimler & Cavonius, 1998; Wachtler, Dohrmann & Hertel, 2004). Moreover, under certain conditions, such as long stimulus presentation and large size of stimuli, dichromats are able to name the color of presented stimuli almost as accurately as normal trichromats (Montag & Boynton, 1987). The precision of dichromatic color naming depends on the size of the stimulus (Smith & Pokorny, 1977), the duration of stimulus presentation (Montag, 1994) and the level of luminance (Paramei et al., 1998).

Not only the color naming behavior of dichromats differs from what is predicted by the reduction hypothesis, contradictory findings come also from other areas of color vision. Smith and Pokorny (1977) report that dichromats do not accept classical dichromatic matches when the size of the stimulus extends to 8° of visual angle. Wavelength discrimination of dichromats is improved at high light levels (McMahon & MacLeod, 1998). Some authors report lower absolute thresholds of dichromats compared to trichromats under scotopic conditions (Verhulst & Maes, 1998) whereas others found no differences (Simunovic, Regan & Mollon, 2001). Morgan, Adam and Mollon (1992) report that dichromats detected color-camouflaged objects that were not detected by normal trichromats. Using a recognition memory task, Gegenfurtner, Wichmann and Sharpe (1998) found that dichromats recognized color images of natural scenes with the same accuracy as normal trichromats.

Several explanations of these findings contradictory to classical reduction hypothesis have been suggested. First, one assumption explaining large field trichromacy of dichromats is the contribution of rods to dichromatic color vision (Smith & Pokorny, 1977; Montag & Boynton, 1987). Second, the improved discrimination and color naming abilities of dichromats may result from the participation of a novel unknown photopigment (Montag, 1994). Third, at very high light levels, S-cones may contribute to discrimination in the long wavelength region as they receive enough light to exceed their threshold (McMahon & MacLeod, 1998).

These three explanations were tested in a study incorporating psychophysical and genetic methods by Crognale, Teller, Yamaguchi, Motulsky and Deeb (1999). When controlling for all three possible mechanisms, the range of large field Rayleigh matches of dichromats was still much smaller than expected. Crognale et al. suggest that this unexpected performance of dichromatic observers might be due to variations in optical density, that means differences in photopigment concentration which may lead to broader sensitivity functions, or due to variations in photopigment concentration across the retina.

An alternative explanation of the extraordinary color naming abilities of dichromatic observers is simply the assumption that dichromats may use learned strategies that increase the probability of correct assignments (Jameson & Hurvich, 1978; Bonnardel, 2006). This does not mean that dichromats necessarily perceive the same distinctive color categories as normal trichromats. We only know that dichromats are able to label presented stimuli more or less correctly but we do not know if different color categories of dichromats are actually related with qualitatively different percepts. However, this explanation can not account for many of the findings discussed above.

A different mechanism that may account for deviations from classical reduction hypothesis is suggested by Wachtler, Dohrmann and Hertel (2004). They propose a non-linear processing of signals from the two remaining cone types which results in a novel spectral response \tilde{Q} . If we consider for example the protanopic case, the \tilde{Q} -response is given by a non-linear transformation of the

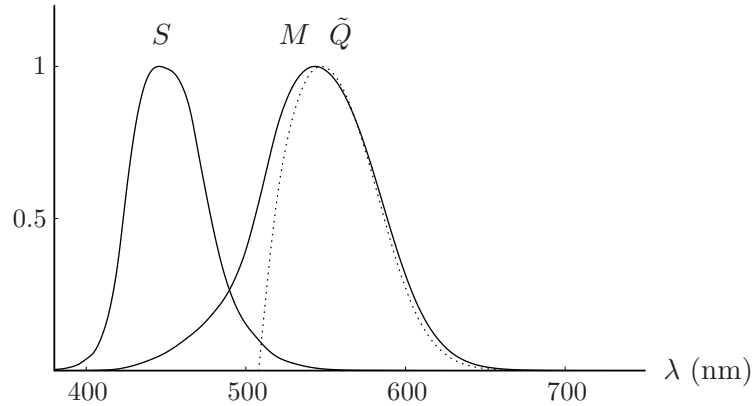


Figure 2.12: Pseudo-trichromatic signals of a protanope as suggested by the model of Wachtler et al. (2004). The solid lines show the sensitivity functions of the two remaining receptors M and S . The dotted line shows the response function of the virtual receptor \tilde{Q} which is given by a non-linear transformation of the M - and S -signals with parameters $\gamma = 1.15$ and $\alpha = 5$.

M -signal minus the weighted signal from the S -cone:

$$\tilde{Q} = M^\gamma - \alpha S, \quad (2.24)$$

where γ is the parameter determining the degree of non-linearity and α the weight of the S -cone signal. Figure 2.12 shows the estimated response function of the virtual receptor \tilde{Q} using parameter values of $\gamma = 1.15$ and $\alpha = 5$ as suggested by Wachtler et al. The authors were able to predict dichromatic hue scalings which were contradictory to the classical theory of dichromacy.¹²

Nonetheless, the model of Wachtler et al. raises several questions. First, it does not seem plausible that a non-linear processing of color signals must be assumed in dichromats but not in trichromats. Second, several well established aspects of dichromatic vision such as confusion lines, the existence of a neutral point or wavelength discrimination are not explained by the model.

To summarize, recent studies have shown deviations from the classical reduction hypothesis of dichromacy in several respects. Explanations that may account for these findings are variations of optical density across the retina and across observers, learned strategies and non-linear processing of signals from remaining cones in order to derive pseudo-trichromatic signals.

2.3 Opponent Colors Theory

2.3.1 Introduction

The trichromatic theory provided a framework within which many phenomena of color vision could be explained. However, critics of this theoretical approach

¹²An introduction to the hue scaling technique is given in Chapter 5.

argued that some phenomena such as afterimages and colored shadows lay beyond the scope of the theory and could not be explained adequately. The most prominent critic of trichromatic theory was Ewald Hering, who developed an alternative theory, the *opponent colors theory* (Hering, 1920). The main idea of this theory is the organization of color perception in pairs of antagonistic colors red-green, blue-yellow and white-black. The two basic colors of each chromatic pair are mutually exclusive which means that color impressions cannot be, for example, bluish and yellowish at the same time. Another important feature of the theory is the assumption that the four basic colors blue, yellow, red and green are conceptualized as *unique hues*. For example, a stimulus which is characterized as uniquely blue appears neither reddish nor greenish to the observer.

At first glance it seems as if the two theories—trichromatic theory and theory of opponent colors—are contradictory. In the late 19th century Helmholtz and Hering were involved in a long debate to decide which one of the two theories could describe human color vision more adequately. Now it is a well established fact that both theories complement one another and refer to two different stages of color processing in the visual system. This idea was already suggested by Johannes von Kries (1905) who integrated both theories within a so called *zone theory*. The main idea of the zone theory is that opponent mechanisms are located at higher stages of color processing and that these mechanisms get their input from the three different types of cones. In neurophysiological studies, neurons which response patterns are in good agreement with opponent colors theory have been found at several levels of the visual pathway (Svaetichin, 1956; De Valois, Abramov & Jacobs, 1966; see Gegenfurtner, 2003 for review).¹³

2.3.2 Quantitative Aspects of the Theory

Jameson and Hurvich (1955) formulated a quantitative version of the opponent colors theory based on psychophysical measurements (see also Hurvich, 1981). They determined experimentally response functions of the two chromatic opponent channels. Based on these measurements of opponent responses they were able to explain several phenomena, such as the Bezold-Brücke shift, wavelength discrimination and color vision deficiencies within the framework of opponent colors theory (Hurvich & Jameson, 1955). In their classical experiment subjects were presented with the mixture of two spectral lights a_λ and b_λ against a black background (Figure 2.13). The wavelength of light a_λ is fixed, but its intensity can be adjusted by the observer. For example, a_λ is chosen as unique blue with $\lambda = 475 \text{ nm}$, which appears neither reddish nor greenish to the observer. The wavelength of the second spectral light b_λ is varied throughout the experiment.

¹³As a matter of fact, the response patterns of opponent cells in the visual pathway do not exactly correspond with the opponent channels proposed by Hering (Krauskopf, Williams & Heeley, 1982; Derrington, Krauskopf & Lennie, 1984). Thus, the neural substrate of unique hues is still to be identified (Valberg, 2001).

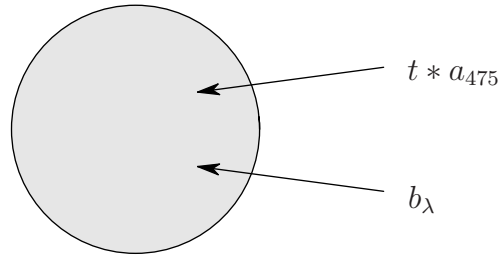


Figure 2.13: Hue cancellation experiment with the spectral light a_{475} as standard.

The task of the subject is to adjust the intensity t of light a_{475} until the mixture c appears neither bluish nor yellowish:

$$c = t * a_{475} \oplus b_{\lambda}. \quad (2.25)$$

In other words, the subject is asked to cancel the blue and the yellow hue from the mixture c . Therefore, this method is also called *hue cancellation*. In the terminology of opponent colors theory the mixture c is in *equilibrium* and the related percepts are called *BY-equilibrium colors*. We can now determine the intensities which are needed to cancel the blue and the yellow hue from the mixture c for all different b_{λ} . As a result we get a response function of the yellow process of the blue-yellow mechanism. If we replace a_{475} by unique yellow a_{580} and measure the amount of yellow across the visible spectrum that is needed to let the mixture appear neither bluish nor yellowish, the result will be the response function of the blue process. Both processes, the blue and the yellow process, complement one another and constitute the response function of the blue-yellow mechanism.¹⁴ By convention the responses of one of the two processes are represented with negative signs.

In the same manner, the response function of the red-green process can be determined by replacing only a_{475} by appropriate spectral lights. In this case, the task of the subject is to adjust the intensity t of the standard a until the mixture c appears neither reddish nor greenish. The response function of the black-white mechanism gives only the ‘whiteness’ response and is identical with the luminous efficiency function (see Figure 2.6). The response functions of the three opponent mechanisms are shown in Figure 2.14.

¹⁴To see this recall that a stimulus can appear only bluish or yellowish. If we use a_{475} as standard and b_{λ} appears also bluish to the observer it is impossible to cancel the blue hue from the mixture. We can only measure a response from the yellow process if the spectral light b_{λ} appears yellowish but not bluish to the observer.

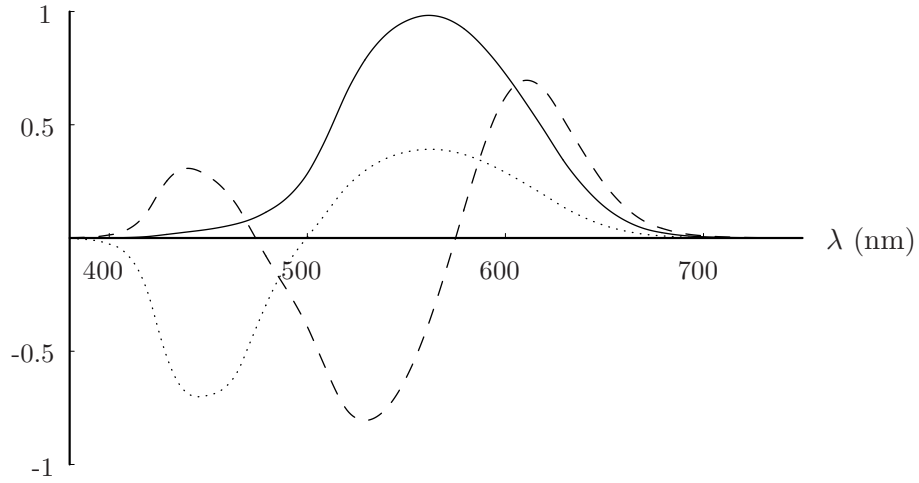


Figure 2.14: Response functions of the three opponent channels blue-yellow (dotted line), red-green (dashed line) and white-black (solid line).

2.3.3 Opponent Color Codes and Relation to Photoreceptor Excitations

Jameson and Hurvich supposed that the responses of the opponent mechanisms are linear functions of photoreceptor excitations. In this case, the *BY*- and the *RG*-equilibria, that is the set of all respective equilibrium colors, can be represented by two different planes in color space (Figure 2.15). The intersection of both planes contains all achromatic colors, the set of colors for which both chromatic mechanisms are in equilibrium. Now I want to introduce opponent color codes $\psi(a) = (\psi_1(a), \psi_2(a), \psi_3(a))$ which give responses of the three opponent mechanisms for each light a . The opponent color codes are defined so that positive and negative codes are possible for the two chromatic mechanisms. Positive and negative signs indicate the activity of one or the other process within each chromatic opponent channel respectively. If we assume the opponent color codes to be linear functions of the stimulus, the following relation must hold for all lights a, b and scalars $s, t \geq 0$:

$$\psi_i(s * a \oplus t * b) = s \cdot \psi_i(a) + t \cdot \psi_i(b); \quad i = 1, 2, 3. \quad (2.26)$$

If we assume (2.26) to be true, we can express the responses of the opponent channels as a linear transformation of photoreceptor excitations. If we denote the response of the *BY*-mechanism for a given light a with $\psi_1(a)$, we can write $\psi_1(a)$ as a linear combination of photoreceptor codes $\phi(a)$ with fixed weights l_{BY} , m_{BY} , s_{BY} :

$$\psi_1(a) = l_{BY} \cdot \phi_1(a) + m_{BY} \cdot \phi_2(a) + s_{BY} \cdot \phi_3(a). \quad (2.27)$$

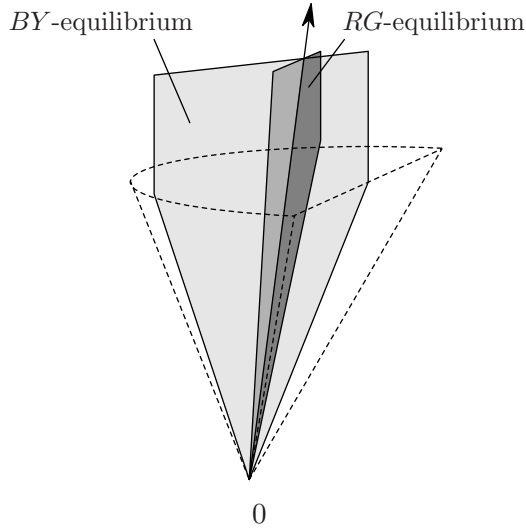


Figure 2.15: *RG*- and *BY*-equilibrium planes in color space. The intersection of both planes (arrow) defines the locus of achromatic colors.

For all *BY*-equilibrium colors the following equation must hold:

$$0 = l_{BY} \cdot \phi_1(a) + m_{BY} \cdot \phi_2(a) + s_{BY} \cdot \phi_3(a). \quad (2.28)$$

The three opponent mechanisms provide a new set of basis vectors of color space. In matrix notation the transformation of receptor codes to opponent color codes can be written as:

$$\begin{pmatrix} \psi_1 \\ \psi_2 \\ \psi_3 \end{pmatrix} = \begin{pmatrix} l_{BY} & m_{BY} & s_{BY} \\ l_{RG} & m_{RG} & s_{RG} \\ l_{WBk} & m_{WBk} & s_{WBk} \end{pmatrix} \cdot \begin{pmatrix} \phi_1 \\ \phi_2 \\ \phi_3 \end{pmatrix}. \quad (2.29)$$

Equation (2.29) can be also interpreted as the linkage between cone receptor output and response of the three opponent mechanisms. This linkage is shown schematically in Figure 2.16. The signs of the coefficients of the transformation matrix in (2.29) indicate if there is an excitatory (+) or an inhibitory (−) relation between one type of cone and an opponent channel. For example, the *BY*-response is given by a weighted sum of the *L*- and *M*-cone signals minus the weighted signal from the *S*-cone as seen in Figure 2.16. The weighting factors of the luminance (or white-black) channel are all positive except s_{WBk} . It is now generally accepted that the *S*-cones do not contribute to luminance and hence $s_{WBk} = 0$ (Eisner & MacLeod, 1980).

In the color cancellation experiment of Jameson and Hurvich (1955) the linearity of the opponent mechanisms as it is stated in (2.26) was not explicitly tested. However, Jameson and Hurvich defined the response functions of the

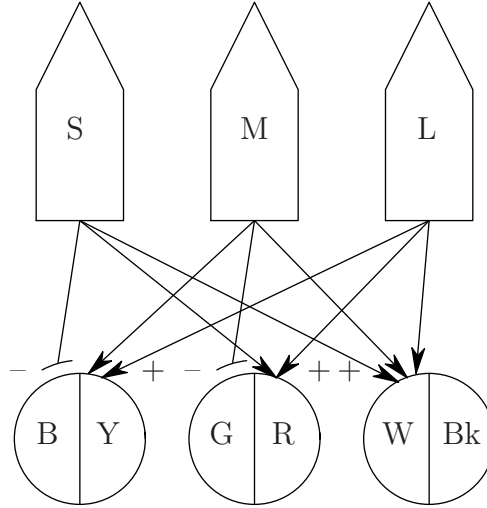


Figure 2.16: Schematic representation of the linkage between cone receptor output and opponent channels. The three photoreceptors are denoted with L , M and S . The signs ‘+’ and ‘-’ indicate excitatory and inhibitory effects respectively.

opponent channels as linear transformations of the color matching functions. Linearity of both chromatic opponent mechanisms was tested experimentally by Larimer, Krantz and Cicerone (1974; 1975). They found that (2.26) holds for the RG -mechanism but not for the BY -mechanism. Further evidence for the non-linearity of the blue-yellow channel comes from experimental studies by Werner and Wooten (1979) and Webster, Miyahara, Malkoc and Raker (2000).

We shall now discuss implications of the opponent theory for red-green deficient dichromats. Exemplarily, we will focus on protanopic vision. Assuming the reduction hypothesis of dichromacy to be true these observers are lacking the L -cone photoreceptors. Therefore, the transformation of receptor codes to opponent signals (see Equation 2.29) reduces to

$$\begin{pmatrix} \psi_1 \\ \psi_2 \\ \psi_3 \end{pmatrix} = \begin{pmatrix} m_{BY} & s_{BY} \\ m_{RG} & s_{RG} \\ m_{WBk} & s_{WBk} \end{pmatrix} \cdot \begin{pmatrix} \phi_2 \\ \phi_3 \end{pmatrix}. \quad (2.30)$$

We note that the transformation matrix has only rank 2. Therefore, the three opponent signals ψ_1 , ψ_2 , ψ_3 contain redundant information. It would be sufficient for the protanope to code signals only in two different opponent channels. One can verify easily that the same is true for deuteranopic observers.

Results from psychophysical studies indicate that protanopes and deuteranopes possess only two different opponent channels which can be characterized as white-black and blue-yellow channel (Hurvich & Jameson, 1955; Knoblauch, Sirovich & Wooten, 1985). The red-green channel is missing in these two classes of observers. The response functions of the protanopic opponent channels are

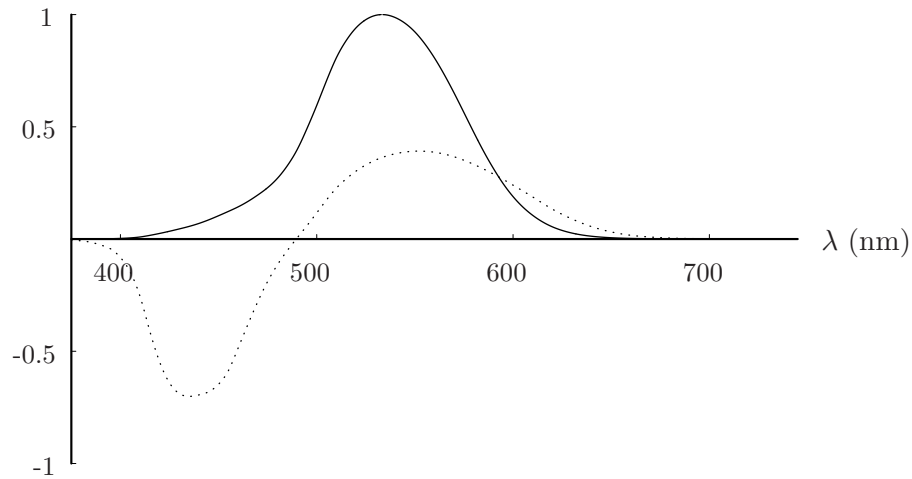


Figure 2.17: Response functions of the two protanopic opponent channels blue-yellow (dotted line), and white-black (solid line). The equilibrium of the BY-channel can be interpreted as the protanopic neutral point. Note that in comparison with Figure 2.14 the response functions are slightly shifted toward the shortwavelength region.

shown in Figure 2.17. Note that due to the lack of L-cone signals response functions are slightly shifted toward the shortwavelength region. The equilibrium of the BY-channel is perceived as achromatic in appearance by the protanope. It can be interpreted as the protanopic neutral point (see Table 2.1).

In Equation (2.30) we assumed silently that opponent signals are a linear function of cone excitations. Results from a study by Knoblauch, Sirovich and Wooten (1985) indicate that linearity of the chromatic blue-yellow channel holds for both protanopes and deuteranopes. This finding is not consistent with detected non-linearities of the blue-yellow channel in normal observers reported earlier.